Shock Dynamics in Shock Turbulence Interaction

B.Tech Project Report

Phase - I

by

Palash Sashittal

10D110002

under the guidance of

Prof. Krishnendu Sinha

Department of Aerospace Engineering

Indian Institute of Technology, Bombay

August 2013

Certificate

This is to certify that this B.Tech project report submitted by Palash Sashittal (Roll No. 10D110002) is approved by me for submission. Certified further that, to the best of my knowledge, the report represents work carried out by the student.

Date: Prof. Krishnendu Sinha

Declaration

I declare that this written submission represents my ideas in my own words. Wherever ideas or words or figures have been included from published works are adequately cited and has been referenced to their original sources. I also declare that I have adhered to all principles of academic honesty and integrity and have not misrepresented or fabricated or falsified data/idea/fact/source in my submission. I understand that any violation of the above will be cause of disciplinary action by the institute and can also evoke penal action from the sources which have thus not been properly cited or from whom proper permission has not been taken when needed.

Date:

Signature:

Acknowledgement

I would like to express my deep sense of gratitude to Prof. Krishnendu Sinha, for his invaluable help and guidance during the course of this seminar work. I am highly indebted to him for constantly encouraging me by giving his critiques on my work and for his thought provoking discussions which inspired me to make this report fruitful. I am grateful to him for having given me his support and time.

I would also like to thank all my fellow lab mates for their kind help and support. I would like to specially thank Mr. Yogesh for always finding time to help me out when I was struggling with anything.

I would like to express my special gratitude to Dr. Johan Larsson, Assistant Professor, Department of Mechanical Engineering, University of Maryland, College Park, USA for all the weekly simulating discussions over skype and DNS data for various cases of canonical shock/turbulence interaction. I am grateful to him for giving me his support and suggestions.

Palash Sashittal
November 2013
Indian Institute of Technology, Bombay

Abstract

Normal shocks have been found to distort upon interaction with turbulence and oscillate about a mean position. This oscillation referred as shock unsteadiness has been observed and studied by both experimentalists and numerical analysts. Understanding the cause of this shock unsteadiness has been deemed necessary to understand the physics of the problem. The cause can either be the fluctuaitons upstream of the shock or downstream of the shock or a combination of both.

In this work, a canonical shock turbulence interaction problem is considered. A theoretical model is developed to explain the physics of shock motion observed in canonical shock turbulence interaction. It is based on conservation of mass across an oscillating shock and a theoretical shock-speed can be obtained from the jump in mass flux across the shock wave. The shock speed thus extracted from DNS data is compared with the time-rate of change of shock location in the simulation. A close match between the two would indicate that the shock motion is primarily governed by one- dimensional phenomena, whereas discrepancies would point towards additional two- and three- dimensional effects. In addition, interaction of one- and two-dimensional plane waves with a normal shock are also considered.

A code is developed to simulate interaction of acoustic wave with normal shock in one dimensional domain. We are trying to investigate if we can reporduce the statistics of the shock-motion in one dimensional simulations by forcing the inflow with broadband fluctuations.

Linear interaction analysis is a analytical tool to study the interaction of linear waves interaction with normal shock. It predicts the generation of left moving acoustic wave downstream of the shock for certain angles of incidence of upstream waves. These waves could also play a role in distorting the normal shock. Two dimensional simulations are conducted to investigate the generation of left moving acoustic waves downstream of the shock.

Keywords: shock turbulence interaction, shock unsteadiness, shock speed, oscillating shock

Contents

List of Figures

Nomenclature

$SBLI$	Shock wave Boundary Layer Interaction
STI	Shock wave Turbulence Interaction
DNS	Direct Numerical Simulation
$RANS$	Reynolds Averaged Navier Stokes
ENO	Essentially Non-Oscillatory
$WENO$	Weighted Essentially Non-Oscillatory
$R-H$	Rankine - Hugoniot
x_1, x_2, x_3	Cartesian coordinates
t	time
T	temperature
p	pressure
ρ	density
u_1	velocity component in (stream wise) x-direction
u_2	velocity component in (normal) y-direction
u_3	velocity component in (span wise) z-direction
γ	ratio of specific heats
ω	vorticity
H	enthalpy
h	specific enthalpy
$\forall$	Volume
ν	kinematic viscosity
M	Mach number
M_t	turbulent Mach number
μ	dynamic viscosity
U	characteristic mean velocity
ξ	shock deviation
ξ_y	angular distortion along y-direction
ξ_z	angular distortion along z-direction
ξ_t	instantaneous shock speed
v_s	assumed constant shock speed
l	turbulence length scale

$\hat{u}$	characteristic turbulent velocity fluctuations
f	other forces such as body, gravitation, etc.
$\vec{V}$	velocity vector
Re	Reynolds number
x_s	shock location
p_{th}	pressure threshold
Subscript u	upstream values
Subscript d	downstream values
$\bar{}$	bar denote Reynolds averaged values
$\tilde{}$	tilde denote Favre averaged values
$'$	prime denote Reynolds fluctuations
$''$	double prime denote Favre fluctuations
$\sim$	varies as (used in order of magnitude analysis)
$\S$	denotes sections

Chapter 1

Introduction

Shock turbulence interactions are common in high speed flows and the dynamics of interaction are widely studied for better design and optimization of aerospace vehicles. Turbulent flow-field interacting with a normal shock wave is one of the simplest cases of shock turbulence interaction and is mostly studied to understand the fundamental physics of such interactions. Still the phenomenon is yet unknown due to the chaotic nature of turbulence and unsteady effects of the shock wave. The very nature of the system is indeterministic because of turbulence but the latter can still be analyzed.

In all cases of supersonic flow in practical applications, shock waves and boundary layers have been the prevalent entities and at sufficiently high Reynolds numbers, the boundary layer becomes turbulent. This problem of Shock wave Boundary Layer Interaction (SBLI) has its roots in Shock Turbulence Interaction (STI) and is thus necessary to be completely understood to answer the questions arising from SBLI cases. Turbulent flow field interacting with normal shock is one of the simplest shock turbulence interaction cases that have been studied extensively in numerical simulations and in experiments to obtain understanding of the fundamental physics that lead to amplification of quantities downstream of the interaction.

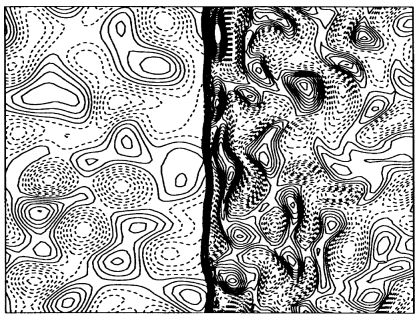

Figure 1.1: Vorticity contour snapshot of $M = 2.0$ shock turbulence interaction case[?]

One of the key features of shock turbulence interaction, mostly studied in shock boundary layer interaction (SBLI) problems is the unsteady motion of the shock. Unsteady shock motion is of engineering interest as it can cause flow separation, changeable heat transfer rates and surface pressure distributions leading to deterioration of the flow quality downstream. DNS

of isotropic turbulence interacting with shock wave, performed by Lee et al.[?] clearly displays the shock distortion due to turbulence in their vorticity contours, seen as a thick wrinkled line in Fig. (1.1). Larsson et al.[2] have also reported of unsteady shock motion affecting Reynolds stresses in a canonical shock turbulence interaction problem. Shock unsteadiness also affects turbulent kinetic energy amplification across the shock[4] which when correctly modeled gives accurate predictions.

There are two major theories that try to explain the cause of unsteady shock motion in SBLI problems. One states that shock unsteadiness is primarily driven by upstream boundary layer and the other states that it is the downstream separated flow that dominantly influences the unsteady shock motion. Ganapathisubramani et al.[11] proposed that incoming turbulent boundary layer is responsible for the low-frequency motion of the shock. Wu and Martin[8] have also observed low frequency oscillations of the shock both in stream-wise and span-wise direction in their DNS study of supersonic flow over turbulent boundary layer in a compression ramp. DNS results by Priebe and Martin[?] on SBLI in compression ramp flow indicate that the stream-wise and span-wise motion of the shock are highly correlated and have claimed that the unsteady shock motion is due to the pulsation of the downstream separated flow. Piponniau et al.[10] developed a simple model to explain the phenomena of low-frequency shock unsteadiness in shock induced separated flows. This model is based on fluid entrainment in the free shear layer enclosing the separation bubble downstream of the shock.

Models have been proposed to account for shock unsteadiness in[4] by modifying the turbulent kinetic energy equation ($k - eqn$) and the solenoidal dissipation rate equation ($\epsilon - eqn$) and this model that has developed on linear analysis, proved to be matching well with available DNS data. Still, the model is applicable for specific cases (such as no gradients in mean flow) and there have been mismatches in turbulent kinetic energy dissipation rates and thus model improvements are necessary. In that line, to develop a better model, a better understanding of the flow physics is deemed necessary.

In this work, model for oscillating shock speed has been attempted based on linear theory assumptions. The governing equations are linearized and a simple formulation has been developed for computing shock speed. Hypothesis of shock moving with constant strength has been proposed to justify the approximations. DNS data shock speed has been calculated using linear interpolation of the pressure profiles and the theoretical shock speed has been calculated by finding the shock location using the highest negative dilatation point. Shock speeds measured from DNS data has been compared with the theoretical formulation and are found to be qualitatively similar.

A code is developed to simulate interaction of acoustic wave with normal shock in one dimensional domain. We are trying to investigate if we can reporduce the statistics of the shock-motion in one dimensional simulations by forcing the inflow with broadband fluctuations. Energy density distribution of the upstream distubances in canonical shock turubulence interaction simulation performed by Dr. Johan Larsson is computed. This distribution will be used in forcing a broadband inflow condition in the code.

We study the generation of left moving acoustic wave downstream of the shock by simulating shock/vorcity-entropy waves interaction in two dimensional domain. Different intial conditions are considered to cover all the regimes of flow predicted by Linear Interaciton Analysis (LIA). Grid convergence study is performed to ensure reliability of the results. A sponge layer is extended at the outflow boundary to create a non-reflecting boundary.

The report has been organized as follows,

- Chapter 2 describes the one dimensional model developed and shows how it compares to simulation data.
- Chapter 3 describes the code developed to study one dimensional interaction of acoustic wave with normal shock and presents preliminary results
- Chapter 4 describes the simulation results for two dimensional interaction of normal shock with vorcity-entropy wave.

Chapter 2

Theoretical shock speed model

2.1 Introduction

We propose a simple one-dimensional model to explain the physics of shock motion observed in canonical shock turbulence interaction. It is based on conservation of mass across an oscillating shock and a theoretical shock-speed can be obtained from the jump in mass flux across the shock wave. The shock speed thus extracted from DNS data is compared with the time-rate of change of shock location in the simulation. A close match between the two would indicate that the shock motion is primarily governed by one- dimensional phenomena, whereas discrepancies would point towards additional two- and three- dimensional effects. We consider different normal shock/homogeneous turbulence interaction cases with varying shock strength and upstream turbulent intensity. In addition, interaction of one- and two-dimensional plane waves with a normal shock are also considered.

Section 2 describes the theoretical formulation for shock speed which is used as a measure for understanding shock motion. Section 3 applies the proposed model numerically on the DNS data and discusses its limitations. Section 4 portrays the preliminary results obtained from comparing the simple model with existing data. Section 5 outlines the proposed work.

2.2 Theory

To estimate the shock speed in a turbulent flow-field, a simple case of one-dimensional (hereby referred to as 1D) normal shock interacting with the flow-field is considered. Note that the quantities are only functions of one spatial direction (x in this case) and time (denoted by t). The Euler equation for mass conservation in 1D is systematically reduced to obtain a simple expression for speed of the shock oscillating about a mean position. The unsteady governing equation in the inertial frame of reference is given by,

$$\frac{\partial \rho}{\partial t} + \frac{\partial (\rho u)}{\partial x} = 0 \tag{2.1}$$

where ρ is the density, u is the velocity of the flow field.

In the frame attached to the unsteady shock wave, the equation is given by

$$\frac{\partial \rho}{\partial t} + \frac{\partial (\rho \acute{u})}{\partial x} = 0 \qquad \text{where,} \quad \acute{u} = u - u_s \tag{2.2}$$

where, u_s is the unsteady shock velocity. It is to be noted that Eq. (2.2) is written in a non-inertial frame of reference.

The temporal variation at a point in this frame of reference will primarily be due to the turbulent fluctuations convected by the mean flow. Thus, the time derivative is of the order of U/l, where U is the characteristic mean velocity and l is the smallest turbulent length scale. This term is small compared to convection across the instantaneous shock thickness δ which scales as U/δ, since $\delta << l$. Thus Eq. (2.2) simplifies to,

$$\frac{\partial (\rho \acute{u})}{\partial x} = 0 \tag{2.3}$$

On comparison of Eq. (4.3) and Eq. (2.3),

$$\frac{\partial \rho}{\partial t} = -u_s \frac{\partial \rho}{\partial x} \tag{2.4}$$

A physical interpretation can be deduced by noting that the density is being convected with the speed of the shock. This implies that temporal change at a fixed point is due to the unsteady shock motion. In a control volume sense, the density of the fluid inside the control volume changes corresponding to the changes in mass flux caused due to the shock unsteadiness in that volume.

2.3 Numerical implementation

DNS data of canonical shock turbulence interaction[1] has been used for analyzing the unsteady shock motion. Three cases of constant Reynolds number based on Taylor micro-scale with varying Mach numbers and turbulent Mach numbers as given in Table 2.1 have been used in this work. These parameters have been taken just upstream of the shock and the domain considered is smaller than in Ref.[1], since the effects around the shock are only of significance in this study.

Shock speed is computed from the DNS data by finding the instantaneous shock location and computing its change in time. We choose a fixed threshold value as the average of the mean values upstream and downstream of the shock and approximate shock location as the point where the shock profile crosses the threshold. Linear interpolation of values just above and below the threshold computes the instantaneous shock location. This imposes the condition that temporal derivative at the shock location is zero in the frame attached to the shock.

Table 2.1: List of DNS cases used in present study and correlation coefficients
RMS denotes root mean square.

	Re_λ	M	M_t	Domain size	$\overline{u_s^{DNS}}$	$\overline{u_s^{Theory}}$	u_s^{DNS} RMS	u_s^{Theory} RMS	Correlation
Case 1	40	1.5	0.16	241×256^2	0.002	0.059	0.595	0.525	0.85
Case 2	40	1.5	0.38	241×256^2	0.011	-0.574	1.412	5.616	0.44
Case 3	40	3.5	0.16	316×256^2	-0.003	-0.017	0.435	0.334	0.88

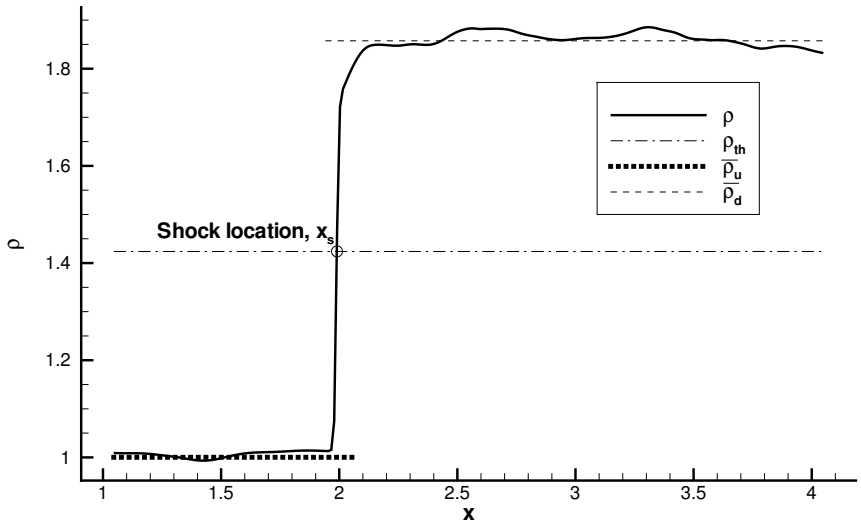

Figure 2.1: Identification of shock location

DNS shock speed is given by,

$$u_s^{DNS} = \frac{\Delta x_s}{\Delta t} \tag{2.5}$$

where, $\Delta x_s = x_s^2 - x_s^1$ denote the movement of shock in the time $\Delta t = t_2 - t_1$. Superscripts denote the time instant in which the shock location was calculated. The shock locations have been calculated using a fixed threshold value and would vary when different threshold values are used.

Theoretical shock speed is obtained from Eq. (2.4),

$$u_s^{Theory} = -\left(\frac{\partial \rho}{\partial t}\right) \Big/ \left(\frac{\partial \rho}{\partial x}\right) \tag{2.6}$$

The numerical implementation of the theoretical formulation on the DNS data is performed by taking the temporal derivative at a point just above the threshold value (which was also used for identification of shock location) and the spatial derivative is taken between points just above and below the threshold value. This implementation as seen in Figs. (2.6,2.8) fails to match exactly with the DNS speed which is the best possible approximation of true shock oscillation speed. Reason is that the shock changes its discrete location (or grid point) and thus

the derivatives are not computed using the same grid points between consecutive time instances.

Theoretical shock speed is computed with values from locations near to the linearly interpolated shock location and thus differ from DNS shock speed. Refer Fig. (2.2) for a geometrical explanation on this issue. Point A of the triangle denote the location just below the threshold (i^{th} point) and point C denote the location just above the threshold (i.e. $(i+1)^{th}$ point) with the distance AB denoting the displacement of the shock in time Δt. The temporal derivative in this case in taken at known locations rather than on exact locations. A' is the point in-between i and $i+1$ that falls under the threshold line for the n^{th} time profile and B' be the point for $(n+1)^{th}$ time profile. A similar triangle can be drawn as mentioned above and the length $A'B'$ would provide the actual displacement of the shock for this threshold value. Ideally, the temporal derivative should be calculated between points C' and B' (which lie on the threshold line) for exact shock speed. Identification of the values at these points is possible only by interpolation and thus requires modification in the expression.

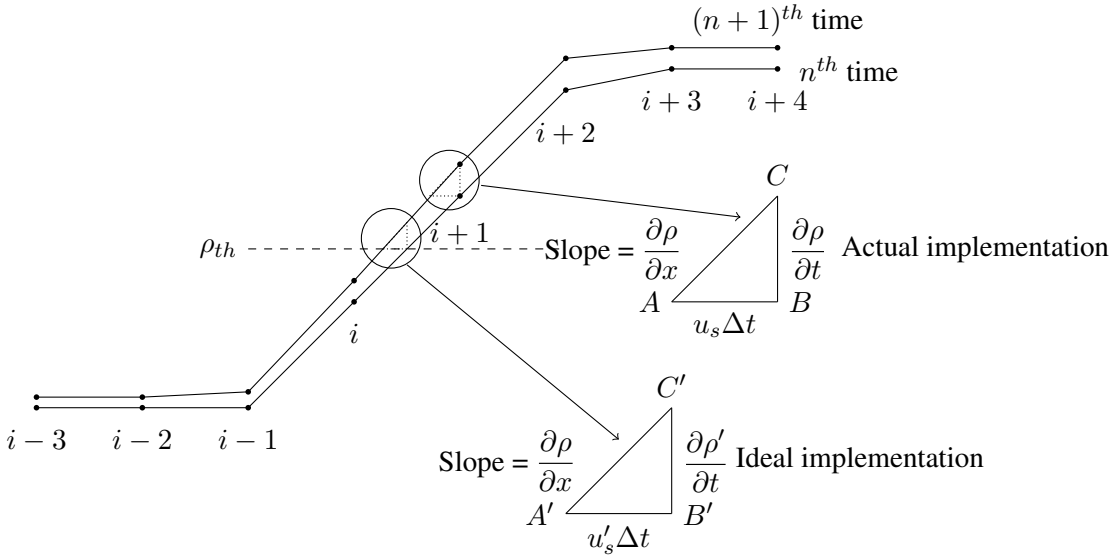

Figure 2.2: Geometrical view of implementation of shock speed formulation Eq. (2.6)

Exact matching of this model with the DNS speed is possible when using weights on the derivatives. It is necessary that a good understanding of the flow profiles is needed in prior to choose proper weights on the derivatives to ensure match between the DNS and theoretical shock speeds. Three possible cases of shock movement in the numerical space have been considered. Fig. (2.3) is an illustration of the case of shock being at the same grid points for two consecutive time instances. Similar illustrations can be made for the cases of shock moving to the next grid point or to the previous grid point in two consecutive time instances as shown in Figs. (2.4a,2.4b).

Following are the terms that would be used in the expressions for modified theoretical formulation for shock speed. The weights, which are made with the help of Figs. (2.3,2.4a,2.4b) as fractions of length of the curves, are denoted as f' in the modified expressions. Here again,

the superscripts denote the time instances and the subscripts denote the spatial locations.

$$\Delta x^1 = x_2^1 - x_1^1 \qquad \Delta x^2 = x_2^2 - x_1^2$$
$$\Delta \rho^1 = \rho_2^1 - \rho_1^1 \qquad \Delta \rho^2 = \rho_2^2 - \rho_1^2$$

When shock is not changing grid points (i.e. its discrete location),

$$u_s^{Theory} = -\left(\frac{\Delta x^1}{\Delta \rho^1}\right)\left[f'\left(\frac{\rho_2^2 - \rho_2^1}{\Delta t}\right) + (1-f')\left(\frac{\rho_1^2 - \rho_1^1}{\Delta t}\right)\right] \qquad f' = \frac{\rho_{th} - \rho_1^2}{\Delta \rho^2} \tag{2.7}$$

When shock is changing grid points and moving forward,

$$u_s^{Theory} = -\left(\frac{\rho_1^2 - \rho_2^1}{\Delta t}\right)\left[f'\left(\frac{\Delta x^1}{\Delta \rho^1}\right) + (1-f')\left(\frac{\Delta x^2}{\Delta \rho^2}\right)\right] \qquad f' = \frac{\rho_2^1 - \rho_{th}}{\rho_2^1 - \rho_1^2} \tag{2.8}$$

When shock is changing grid points and moving backward,

$$u_s^{Theory} = -\left(\frac{\rho_2^2 - \rho_1^1}{\Delta t}\right)\left[f'\left(\frac{\Delta x^2}{\Delta \rho^2}\right) + (1-f')\left(\frac{\Delta x^1}{\Delta \rho^1}\right)\right] \qquad f' = \frac{\rho_2^2 - \rho_{th}}{\rho_2^2 - \rho_1^1} \tag{2.9}$$

Exact matching of this modified formulation with DNS data have been shown as symbols in Figs. (2.6,2.8)

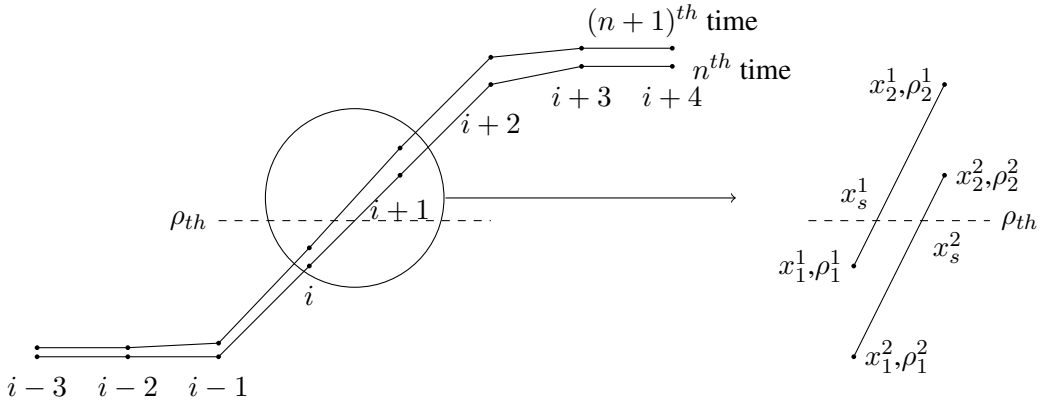

Figure 2.3: Illustration of shock being at the same point. Superscripts 1 and 2 denote the values from time t_1 and t_2 respectively and subscripts 1 and 2 denote the discrete spatial locations. ρ_{th} is the threshold line.

The shape of the shock is a numerical manifestation rather than a physical feature in numerical simulations. The unsteady shock physics can be better explained if the shock speed is computed away from a numerical shock.

On comparison of Eq. (4.3) and Eq. (2.4),

$$u_s \frac{\partial \rho}{\partial x} = \frac{\partial (\rho u)}{\partial x} \tag{2.10}$$

The following relation between shock speed and flow variables across the shock is obtained

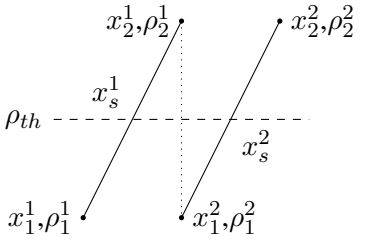

(a) Shock moving forward

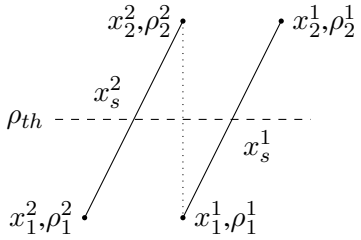

(b) Shock moving backward

Figure 2.4: Other possible cases of shock oscillation.

by integrating this conservative equation :

$$u_s = \frac{[\rho u]}{[\rho]} \tag{2.11}$$

where, [ ] denotes jump across shock.

The above is same as the Rankine-Hugoniot (R-H) conditions for a moving shock wave. Shock speed thus obtained is denoted by u_s^{RH}. Further analysis needs to be carried out in this regard.

2.4 Preliminary results

Shock speed computed from the three major cases (Table 2.1) are shown in Figs. (2.6,2.7,2.8). The legend in these figures define the shock speed computed using the expressions as described below:

- DNS – DNS expression Eq. (2.5)
- Basic formulation – Theoretical expression Eq. (2.6)
- Modified formulation – Modified expressions Eq. (2.7,2.8,2.9) depending on the flow profile.

It is clearly observed that the theoretical expression depends on the identification of the closest points to the fixed threshold value to obtain a better estimation. The theoretical expression seems to match well for points that have been identified closest to the threshold and fail to match for points that are relatively far apart from the threshold line. The capturing of the points inside the shock structure is essential for computing the derivatives.

Fig. (2.5) displays the variation of 1D sinusoidal acoustic plane wave interacting with a normal shock. The flow field parameters are Mach number, $M = 1.5$, wave number, $k = 1$ and the amplitude of the pressure fluctuations is 1% of the mean. It is seen that the proposed model always underestimate the shock speed for this case. The correlation coefficient for the shock speeds computed from the DNS and theoretical expressions for the 1D simulation of plane wave

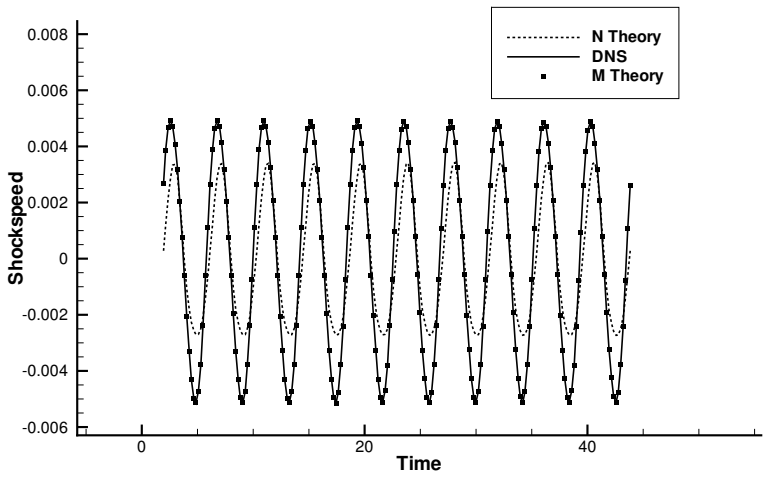

Figure 2.5: Shock speed variation in time for a plane wave interacting with a normal shock

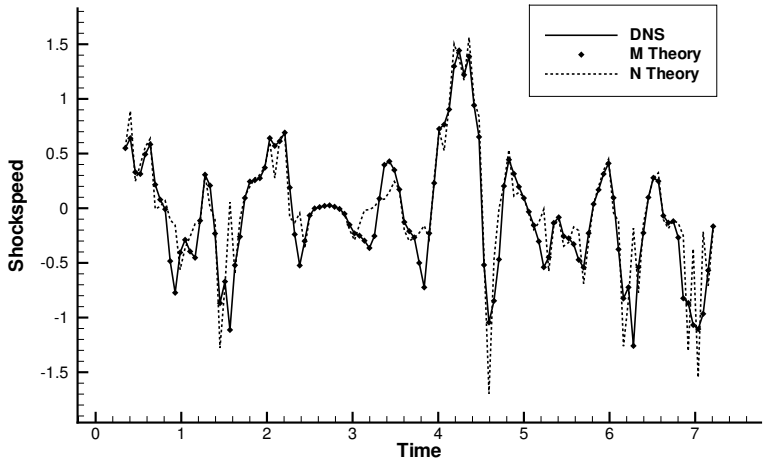

Figure 2.6: Shock speed variation in time for $M = 1.5$ $M_t = 0.16$ case

interacting with a normal shock was 0.93 which is quite high implying that the proposed model is comparably capturing the physics of the problem.

Correlation between the DNS expression Eq. (2.5) and theoretical expression Eq. (2.6) are tabulated in Table 2.1. Shock speed computed from the modified expression exactly matches for Cases 1 and 3 but not for Case 2. Case 2 is of broken shock regime caused due to intense upstream turbulence. It is difficult to identify the shock location with a fixed threshold on a particular plane for this broken shock case. Thus, the modified expression would require different weights to account for this special case. The correlation coefficients are high enough to show that the shock speed computed from theoretical expression is comparable to that of the DNS expression.

The drop in correlation coefficient for high M_t case can be explained by two things. Firstly, the model is based on the assumption that temporal change at a point due to turbulence being convected by mean velocity is small compared to the change due to unsteady shock motion. At

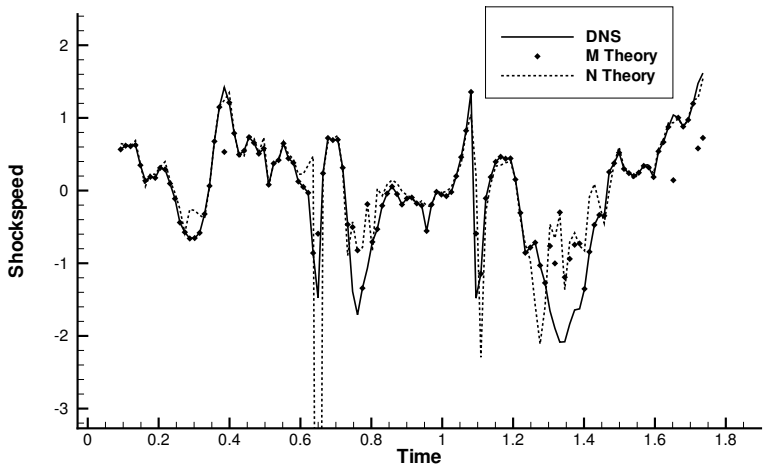

Figure 2.7: Shock speed variation in time for $M = 1.5$ $M_t = 0.38$ case

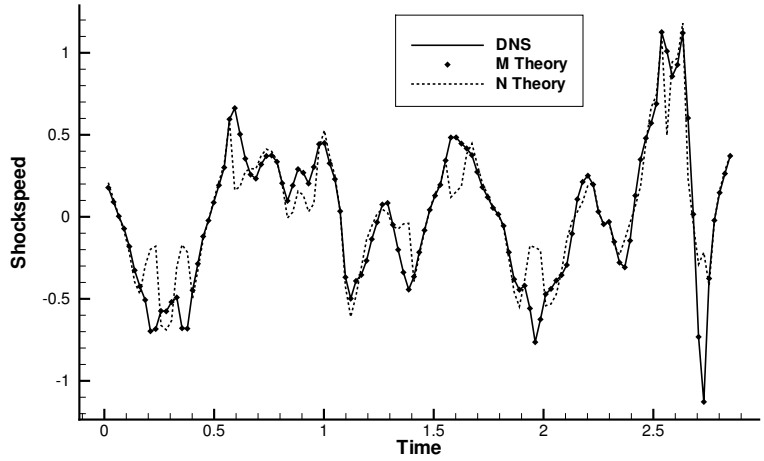

Figure 2.8: Shock speed variation in time for $M = 3.5$ $M_t = 0.16$ case

high M_t this assumption is not true. Secondly, as mentioned above, this case falls in the broken shock regime which means that formation of shock holes occurs. Our model will not be valid at the points where the shock breaks.

2.5 Proposed work

Shock speed will be determined using the model expression and DNS expression from simulations of 1D and 2D plane waves interacting with a normal shock. The computed shock speeds will be compared with shock speed computed from DNS data to study the dominant effects causing unsteady shock motion. An attempt will be made to understand if the mechanisms causing shock unsteadiness are one-dimensional or multi-dimensional.

The R-H form of the shock speed will be compared with DNS shock speed and validated of their physical relevance by taking the jump of flow variables across the shock. This would be

more reasonable since the shock is found to be changing in strength (seen as change of slope) in its entire structure.

Budget analysis on the mass conservation equation will be performed to support the study of dominant effects of unsteady shock motion. The governing equation is broken into linear and non-linear terms and the effects of each term can be studied on the unsteady shock motion. It is possible to compare shock speed from linear terms using Linear Interaction Analysis (LIA). This helps in understanding the contribution of non-linear terms on shock unsteadiness.

Chapter 3

One dimensional numerical experiments

3.1 Governing Equations

The governing equations solved are one dimensional euler equations based on principles of conservation of mass, momentum and energy written as follows,

$$\frac{\partial \rho}{\partial t} + \frac{\partial \left(\rho u_1\right)}{\partial x_1} = \sigma(\rho_{ref} - \rho) \tag{3.1}$$

$$\frac{\partial \rho u_1}{\partial t} + \frac{\partial \left(\rho u_1^2 + p\right)}{\partial x_1} = \sigma(\rho u_{ref} - \rho u) \tag{3.2}$$

$$\frac{\partial E}{\partial t} + \frac{\partial \left(\left(E + p\right) u_1\right)}{\partial x_1} = \sigma(E_{ref} - E) \tag{3.3}$$

where, E is total energy per unit volume given by $\rho e + \frac{1}{2}\rho(u_1^2)$, rho is density, u_1 is components of velocity in x_1 direction, p is pressure and e is internal energy.

Gas is assumed to be calorically perfect with $\gamma = 1.4$ and follows the ideal-gas law given by

$$P = \rho RT \tag{3.4}$$

3.2 Initial and Boundary Conditions

The computaitonal domain is streched from x=-5 to x=5. A Reimann problem for a case of $u_l < u_r$ is considered. It can be noticed that a shock is introduced at x=0. The initial conditions are given so that they satisfy Rankine-Hugoniot jump conditions which are as follows :

$$(\overline{\rho}, \overline{u}, \overline{p}) = \begin{cases} (\rho_L, u_L, p_L) = (1, 1.5, 0.714286)\,, & x < 0, \\ (\rho_R, u_R, p_R) = (1.8862069, 0.805556, 1.755952)\,, & x > 0. \end{cases} \tag{3.5}$$

and the conditions at the inflow boundary x=0 are

$$\begin{aligned} \rho &= \rho_L + \rho_L \frac{A_p}{\gamma} sin((u_L + a_1)t), \\ u_1 &= u_L + u_L \frac{A_p}{\gamma M_1} sin((u_L + a_1)t), \\ p &= p_L + A_p sin((u_L + a_1)t). \end{aligned} \tag{3.6}$$

where, A_p is taken as 0.01. The right boundary conditions are used to fix the drifting shock in space. This is dicussed in the next section.

3.3 Fixing Shock in Space

When upstream disturbances approach a normal shock, one of the difficulties faced is the drifting of shock. Apart from oscillating about its mean position, the mean position of the shock itself begins to move. This causes variation of upstream Mach number contiously with time and it becomes difficult to validate the results for a pre-defined upstream Mach number. Moreover, if the shock is not made stationary it could move out of the domain if the simulation is run logn enough. In this section, an approach towards fixing the shock in space is discussed. This method allows us to evaluate the model and results without the variation of inlet conditions with time.

In order to stop the drifting of the shock without affecting the flow topology, an integral controller is incorporated in the outflow boundary condition. It is similar to controlling the back pressure of the outflow to make the shock stationary.

We control the characteristic variable corresponding to left moving wave, the wave with speed $u - a$. We use an integral controller with instantaneous shock velocity as input variable. The following control law is used

$$V_{bc}^{n+1} = V_{bc}^{n} + ki \frac{\triangle t}{T} \int_{t-T}^{t} u(\tau) d\tau \tag{3.7}$$

where, k_i is a controller constant whose value determines the time taken by the system to reach steady state. Different values of k_i where tried and 0.015 was chosen since it gave a good convergence rate.

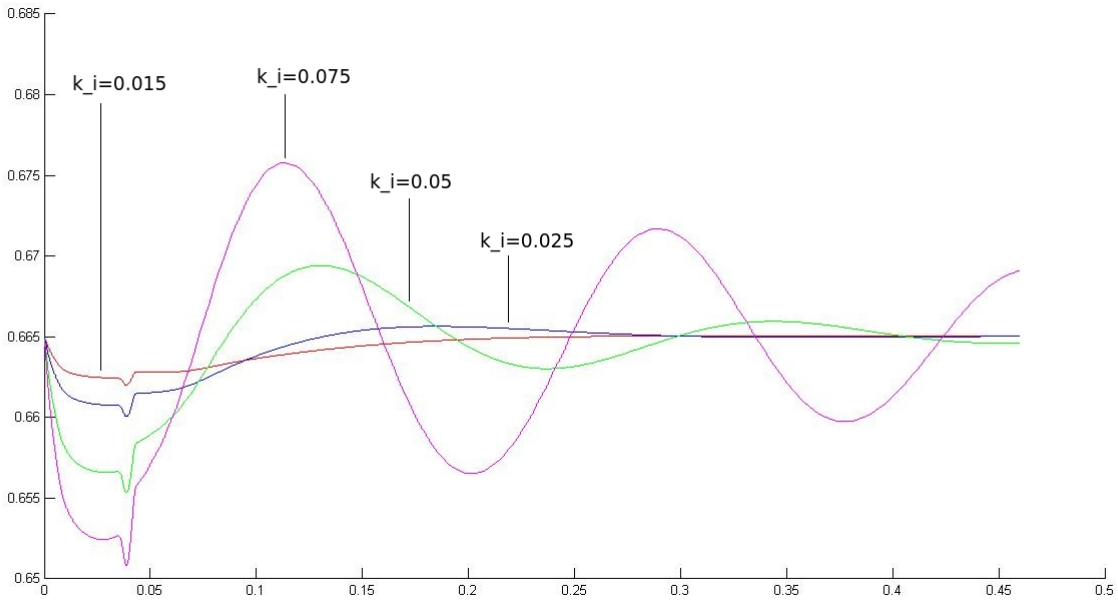

Figure 3.1: Boundary condition variation with time for various values of integral constant

3.4 Numerical Scheme and Simulation Methodology

The numerical scheme used to solve the spatial derivaties is Lax-Friedrich scheme which is given by,

$$U_j^{n+1} = \frac{1}{2}(U_{j+1}^n + U_{j-1}^n) - \frac{\alpha k}{2h}(U_{j+1}^n + -U_{j-1}^n) \tag{3.8}$$

Time marching is handled using a standard fourth order Runge-Kutta scheme. This method gives freedom of using higher CFL values. For linear problems this method is stable for $CFL \leq 2.8$.

3.5 Grid Refinement

Initially a grid with 501 baseline points was used and gradually increased towards 10000 points until a grid converged solution is obtained. The grid points are equally spaced and stretching of grid is not performed. Shock location and shock speed are the variables used to study grid convergence.

3.6 Energy density distribution

A canonical isotropic turbulence interaction with a normal shock at $M = 1.5$ and $M_t = 0.16$ is taken into consideration to compare with the one dimensional simulation results. Energy density

distribution of upstream turbulent energy is computed with respect to wavenumber. Data points are taken three grid points ahead of the mean shock.

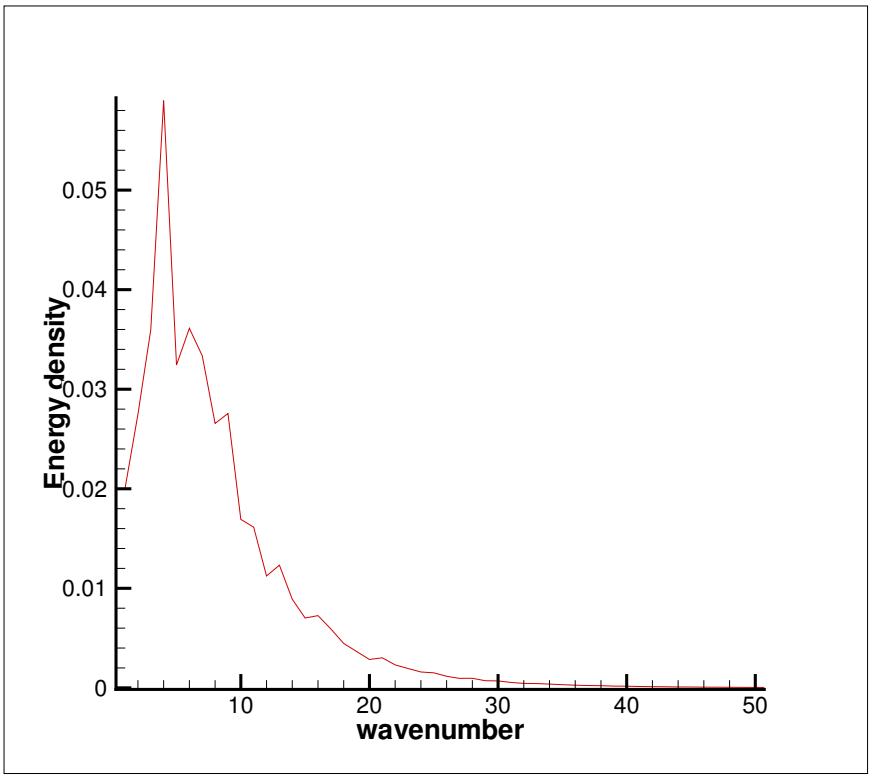

Figure 3.2: Energy density spectrum for upstream turbulence

The inflow coditions for one dimensional simulations will be set to mimic the energy distribution of isotropic turbulence. Shock dynamics thus extracted will be compared with direct numerical simulation data.

3.7 Future work

Simulations will be run with required upstream energy distribution to compare with direct numerical simulation data. Close comparison will indicate that shock dynamics of three dimensional shock turbulence interaction can be reproduced by one dimensional simulation. Thorough investigation will be conducted to study its dependence on upstream Mach number and turbulent Mach number.

Chapter 4

Shock-vortictiy/entropy interaction

Two dimensional shock-vorticity/entropy interaction simulations are performed. Code developed by Dr. Johan Larsson is used for these simulation and slight modifications are made in the code wherever required.

4.1 Linear interaction analysis

Linear interaction analysis (LIA) is an analytical tool used to study the interaction of vorticity-entropy wave with a normal shock. Complete solution for downstream flow field can be found in linear limit using LIA. Ratio of wavenumber for downstream acoustic wave to upstream vortical-entorpy wave can be found as a function of incidence angle of disturbance and the Mach number of the shock wave.

It is found that for certain angle of incidence at a given Mach number, the acoustic wave generated downstream starts moving to the left (towards the shock) rather than towards the outflow. This left moving acoustic wave could influence the shock dynamics. Considering that the wave downstream are generated at the shock, it is important to understand the mechanism by which a left moving acoustic wave could be generated.

4.2 Governing Equations

We solve two dimensional Euler equations based on conservation of mass, momentum and energy which are as follows,

$$\frac{\partial \rho}{\partial t} + \frac{\partial \left(\rho u_1\right)}{\partial x_1} + \frac{\partial \left(\rho u_2\right)}{\partial x_2} = 0 \tag{4.1}$$

$$\frac{\partial \rho u}{\partial t} + \frac{\partial \left(\rho u_1^2 + p\right)}{\partial x_1} + \frac{\partial \left(\rho u_2^2 + p\right)}{\partial x_2} = 0 \tag{4.2}$$

$$\frac{\partial E}{\partial t} + \frac{\partial \left(\left(E + p\right) u_1\right)}{\partial x_1} + \frac{\partial \left(\left(E + p\right) u_2\right)}{\partial x_2} = 0 \tag{4.3}$$

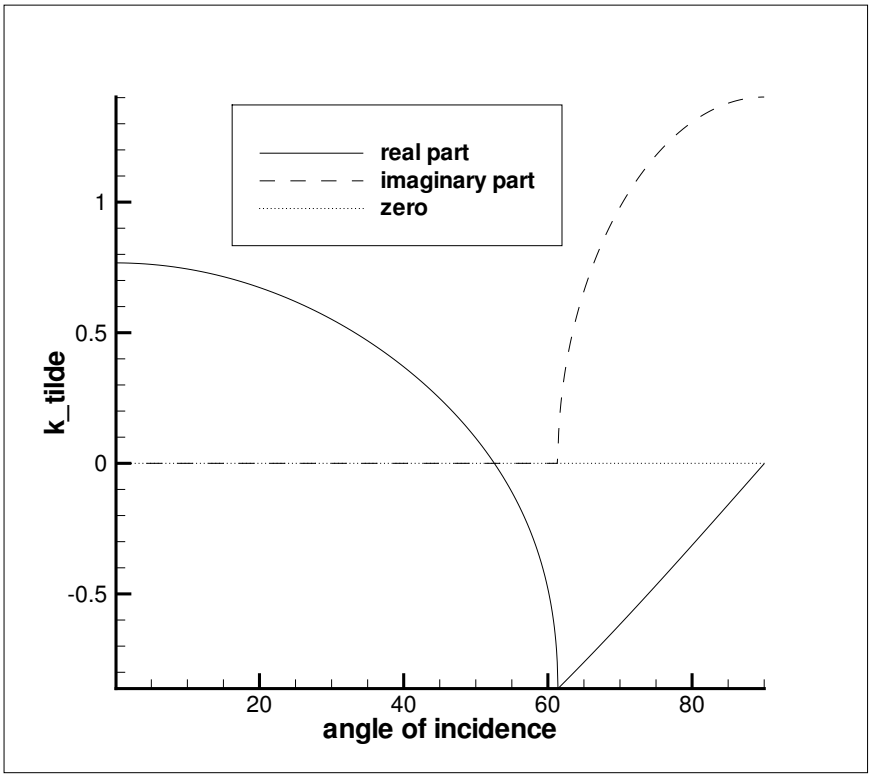

Figure 4.1: Downstream acoustice wave's wave number as function of angle of incidence of upstream disturbance

where, E is total energy per unit volume given by $\rho e + \frac{1}{2}\rho(u_1^2 + u_2^2)$, rho is density, $u_1 and u_2$ are components of velocity in $x_1 and x_2$ directions respectively, p is pressure and e is internal energy.

Gas is assumed to be calorically perfect with $\gamma = 1.4$ and follows the ideal-gas law given by

$$P = \rho RT \tag{4.4}$$

4.3 Numerical framework

The code consists of a seventh-order accurate conservative finite difference WENO scheme for the interpolation, Roe flux splitting with entropy fix for upwinding and a carbuncle fix. The time-marching is handled using a standard fourth-order accurate Runge-Kutta scheme.

4.4 Initial and boundary conditions

The upstream disturbances consist of a single vorticity-entropy wave. Periodic boundary conditions are used in y direction; x=0 is a supersonic inflow and $x = 4\pi$ is a subsonic outflow. Different techniques are employed to avoid acoustic reflection from the outflow, including an

extension of the domain with a sponge region. First a one-dimensional base solution corresponding to a $M = 1.5$ shock is defined as

$$(\overline{\rho}, \overline{u}, \overline{p}) = \begin{cases} (\rho_L, u_L, p_L) = (1, 1.5, 0.714286)\,, & x < 3\pi/2, \\ (\rho_R, u_R, p_R) = (1.8862069, 0.805556, 1.755952)\,, & x > 3\pi/2. \end{cases} \tag{4.5}$$

and the conditions at the inflow boundary x=0 are

$$\begin{aligned} \rho &= \overline{\rho} + \rho_L A_e cos(k_2 x_2 - k_1 u_L t), \\ u_1 &= \overline{u}_1 + u_L A_v sin\psi cos(k_2 x_2 - k_1 u_L t), \\ u_2 &= -u_L A_v cos\psi cos(k_2 x_2 - k_1 u_L t), \\ p &= p_L. \end{aligned} \tag{4.6}$$

where,

$$k_1 = \frac{k_2}{tan\psi}, A_e = A_v = 0.001, \tag{4.7}$$

and $k_2 = 1.2$. This inviscid problem has no length scale other than k_2; hence an increase of k_2 corresponds to an effectively coarser grid.

Here, the fluctuations in ρ give rise to convection of entropy wave and velocity fluctuations give rise to convection of vorticity fluctuations from inflow towards the shock.

An extension to the domain with a sponge layer that follows square law with distance is employed at the outflow.

4.5 Preliminary results

To investigate the generation of left moving downstream acoustic waves we need to seperate the acoustic wave from the rest of the flow field. Dilatation is generated by only the acoustic wave hence, we plot dilatation contours for three angle of incidences of upstream distubances, one for each regime that LIA predicts.

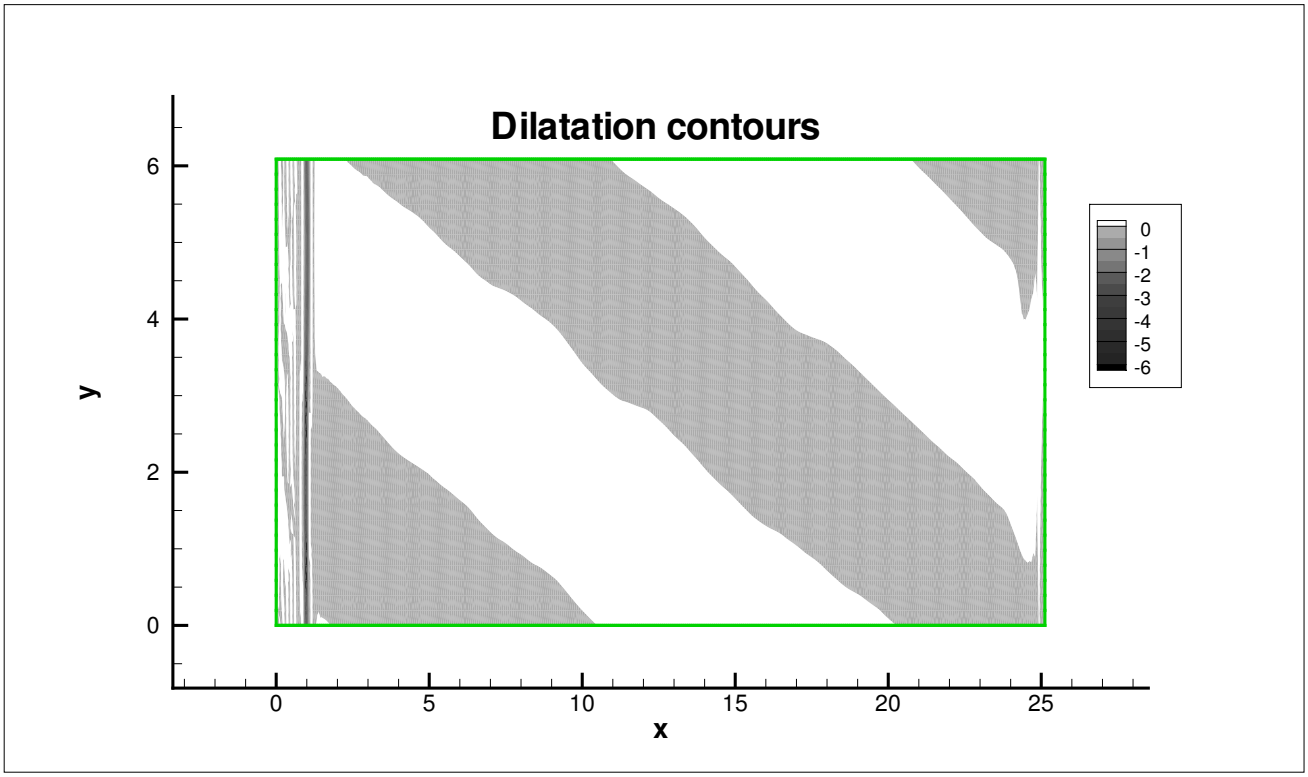

Figure 4.2: Dilatation contours for 45° angle of incidence. The thick dark line at $x = 1$ denote the unsteady shock.

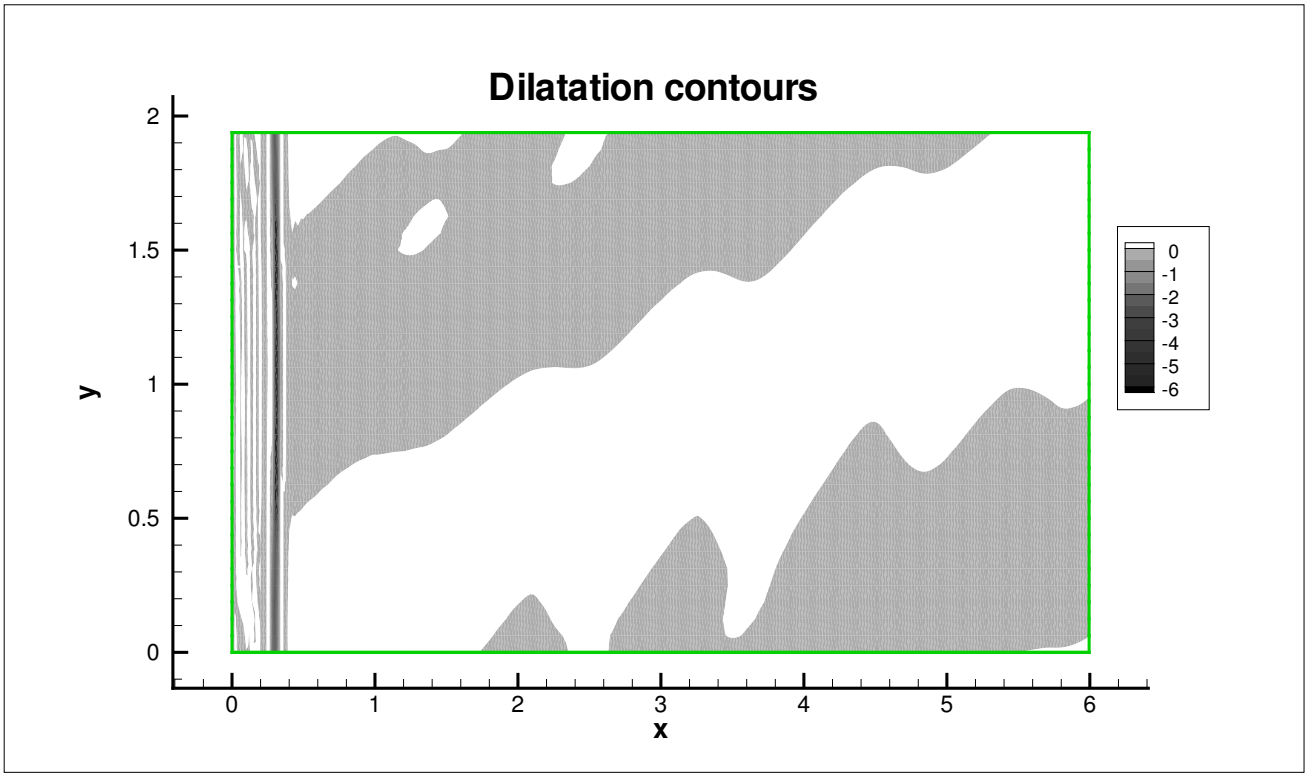

Figure 4.3: Dilatation contours for 45° angle of incidence. The thick dark line at $x = 1$ denote the unsteady shock.

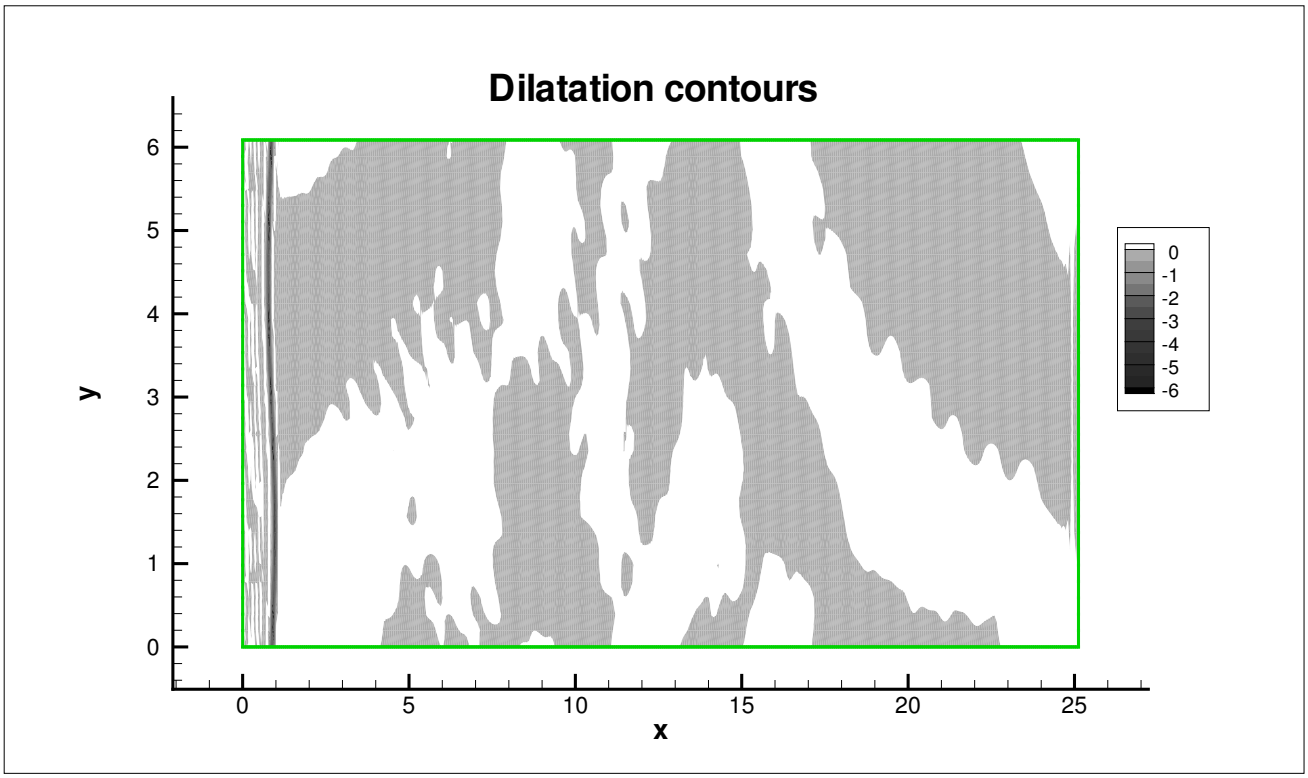

Figure 4.4: Dilatation contours for 45° angle of incidence. The thick dark line at $x = 1$ denote the unsteady shock.

4.6 Future work

Different cases will be run to cover the regimes predicted by LIA and comparison of simulation results will be made with analytical solutions. If left moving acoustic waves are generated downstream of the shock, the underlying mechanism will be investigated.

Chapter 5

Summary

Shock waves in a turbulent environment has been vastly studied but the dynamics of interaction have not yet been completely understood. Literature on shock wave turbulent boundary layer interaction has proved that the shock is oscillating about a mean position due to turbulent fluctuations in the flow field. Previous studies on shock unsteadiness were developed on correlations with fluctuations and modeling coefficients which vary depending on the problem considered.

This work is focused on finding the cause of shock unsteadiness and understanding the mechanisms that influence the shock dynamics when turbulence passes through a normal shock. Both, analytical and numerical approaches are taken into consideration in this investigation which are the following :

A simple formulation for shock speed based on linear theory is proposed. The developed theoretical shock speed computed from simulation data will be compared to actual shock speed computed as rate of change of shock location with time. A close match will indicate that one dimensional mechanisms are primarily responsible for shock unsteadiness and differences will point towards additional two and three dimensional effects.

One dimensional simulation environment is set up to simulate the interaction of planar acoustic wave with normal shock. Energy density distribution of Direct Numerical Simulation (DNS) data of canonical shock/turbulence interaction is carried out which will be used in imposing a broadband inflow condition for one dimensional simulation. The statistics of shock dynamics from this simulation will be compared to DNS data.

Linear interaction analysis (LIA) is an analytical tool used to study interaction of vorticity-entropy waves with normal shock. It predicts the generation of left moving acoustic wave downstream of the shock for some angle of incidences of upstream vorticity-entropy wave. These waves could hit the shock from downstream and influence shock dynamics. Numerical simulations are carried out to investigate the generation of these waves and their effect on the shock.

Bibliography

[1] Larsson, J. and Lele, S. K. "Direct numerical simulation of canonical shock/turbulence interaction", Physics of Fluids, vol. 21, no.12, 126101.

[2] Larsson, J., Bermejo-Moreno, I. and Lele, S. K. "Reynolds- and Mach-number effects in canonical shock-turbulence interaction", Journal of Fluid Mechanics, vol. 717, pp. 293-321, 2013.

[3] Sinha, K. "Evolution of enstrophy in shock/homogeneous turbulence interaction", Journal of Fluid Mechanics, vol. 707, pp. 74-110, 2012.

[4] Sinha, K., Mahesh, K. and Candler, G. V. "Modeling shock unsteadiness in shock/turbulence interaction", Physics of Fluids, vol. 15, no. 8, 2290.

[5] Veera, V. K. and Sinha, K. "Modeling the effect of upstream temperature fluctuations on shock/homogeneous turbulence interaction", Physics of Fluids, vol. 21, no. 2, 025101.

[6] Pasha, A. A. and Sinha, K. "Shock-unsteadiness model applied to oblique shock wave/turbulent boundary-layer interaction", International Journal of Computational Fluid Dynamics, vol. 22, no. 8, pp.569-582, 2008.

[7] Wu, M. and Martin, M. P. "Direct numerical simulation of supersonic turbulent boundary layer over a compression ramp", AIAA Journal, vol. 45, no. 4, pp. 879-889, 2007.

[8] Wu, M. and Martin, M. P. "Analysis of shock motion in shock wave and turbulent boundary layer interaction using direct numerical simulation data", Journal of Fluid Mechanics, vol. 594, pp. 71-83, 2008.

[9] Priebe, S. and Martin, M. P., "Low-frequency unsteadiness in shock wave-turbulent boundary layer interaction", Journal of Fluid Mechanics, vol. 699, pp. 1-49, 2012.

[10] Pipponniau, S., Dussauge, J. P., Debiève, J. F., and Dupont, P., *A simple model for low-frequency unsteadiness in shock-induced separation*, Journal of Fluid Mechanics, Vol. 629, 2009, pp. 87-108.

[11] Ganapathisubramani, B., Clemens, N. T. and Dolling, D. S. "Effects of upstream boundary layer on the unsteadiness of shock-induced separation", Journal of Fluid Mechanics, vol. 585, pp. 369-394, 2007.

[12] Zank, G. P., Zhou, Y., Matthaeus, W. H. and Rice, W. K. M. "The interaction of turbulence with shock waves: A basic model", Physics of Fluids, vol. 14, no. 11, 3766.

[13] Kovasznay, L. S. G. "Turbulence in Supersonic Flow", Jour. Aero. Sci., vol. 20, no. 10, pp. 657-674,682, 1953.

[14] Moore, F. K. "Unsteady Oblique Interaction of a Shock wave with a Plane Disturbance", NACA-TR-1165, 1954. (Supersedes NACA TN 2879, 1953.)

[15] Ribner, H. S. "Convection of a Pattern of Vorticity Through a Shock Wave, NACA-TR-1164, 1954. (Supersedes NACA TN 2864, 1953.)

[16] Anderson Jr., J. D. "Computational Fluid Dynamics: The Basics with Applications", McGraw Hill Series in Mechanical Engineering, 1995.